CHIN.PHYS.LETT. Vol. 25, No. 4 (2008) 1368

Vaporization and Plasma Shielding during High Power Nanosecond Laser Ablation of Silicon and Nickel *

LIU Dan(刘丹)[1], ZHANG Duan-Ming(张端明)[2**]

[1]*Department of Physics and Electronic Engineering, Hubei University of Education, Wuhan 430205*
[2]*Department of Physics, Huazhong University of Science and Technology, Wuhan 430074*

(Received 6 December 2007)

A thermal model to describe the high-power nanosecond pulsed laser ablation is presented. It involves the vaporization and the following plasma shielding effect on the whole ablation process. As an example of Si target, we obtain the time evolution of the calculated surface temperature, ablation rate and ablation depth. It can be seen that plasma shielding plays a more important role in the ablation process with time. At the same time, the ablation depth with laser fluence based on different models is shown. Moreover, we simulate the pulsed laser irradiation Ni target. The evolution of the transmitted intensity and the variation of ablation depth per pulse with laser fluence are performed. Under the same experimental conditions, the numerical results calculated with our thermal model are more in agreement with the experimental data.

PACS: 52. 50. Jm, 79. 20. Ds

For the last two decades, pulsed laser ablation (PLA) of solids has been the subject of increasing research interest owing to expanding applications (film deposition, material processing, cluster and nanostructure production, etc). Despite growing penetration into the processes taking place during PLA, the mechanisms of laser vaporization of materials are still not fully understood, especially in the high-power nanosecond pulsed laser ablation processes.[1,2] When a high-power laser beam (the laser intensity exceeds $10^8\,\mathrm{Wcm^{-2}}$) irradiates on a target surface, the target will absorb the laser energy and the vapour is formed. The vapour becomes significantly ionized, absorbing part of the incident laser beam and leading to vapour breakdown and plasma formation. Then, the plasma will absorb a fraction of the laser light. Vaporization effect and vaporization characteristics generated by laser ablation are neglected by most of the previous work. Kelly and Miotello only present the vaporization phenomenon without studying the effect of vaporization on laser ablation.[3,4] Lu *et al.*[5] and Peterlongo *et al.*[1] partly studied the vaporization effect during the laser irradiation, however, without considering the vaporization effect after the completion of laser irradiation. Our group completely studied the vaporization effect in the whole laser ablation, but neglected the effect of plasma shielding in the ablation process.[6]

In this Letter, we present modelling of high-power nanosecond laser ablation, which not only considers vaporization effect but also involves plasma shielding. As an example of Si target, we obtain the time evolution of the calculated surface temperature, ablation rate and ablation depth. Moreover, we simulate the pulsed laser irradiation Ni target. The time evolution of the transmitted intensity and the variation of ablation depth per pulse with laser fluence are performed. Our numerical results are in good agreement with the experimental data.

The theoretical description of laser-induced target heating and material removal are based on the model proposed in Refs. [7-10]. When the laser intensity is between 10^7 and $10^8\,\mathrm{Wcm^{-2}}$, the model of laser sputtering[1,2,11] has been proven to be accurate. Nevertheless, it is not applicable at high irradiance (the laser intensity exceeds $10^8\,\mathrm{Wcm^{-2}}$). The vapour becomes significantly ionized, Absorbing part of the incident laser beam leads to vapour breakdown and plasma formation. Therefore, we present the model of laser-target interaction, the consequent heat conduction and evaporation process, taking into account the plasma absorption effect. The application of the thermal model can be extended to the whole fluence range of the thermal vaporization regime up to the threshold for phase explosion.

During the pulsed laser irradiation, the optical penetration depth δ_P, ($\delta_P = b^{-1}$, b is the absorption coefficient) is much shorter than the thermal diffuse depth δ_m[2] ($\delta_m = A\sqrt{\alpha\tau}$, α is the thermal diffusion coefficient, A is an alterable coefficient relative to different targets).

The heating and melting processes of pulsed laser irradiation can be simplified into a one-dimensional heat problem.[1,3,11] For convenience, we set the coordinate origin at the ablation surface,

$$C_s\rho_s\frac{\partial T_s}{\partial t} = \frac{\partial}{\partial x}\Big(K_s\frac{\partial T_s}{\partial x}\Big) + (1-R)\alpha_b I(t)\exp(-\alpha_b x), \quad (0 < t \le \tau_m, \quad 0 < x \le \delta_m), \tag{1}$$

*Supported by the National Natural Science Foundation of China under Grant No 50272022, the Natural Science Foundation of Huibei Province under Grant No 2001ABB099, and Sunshine Foundation of Wuhan City under Grant No 20045006071-40.

**To whom correspondence should be addressed. Email: zhangd@public.wh.hb.cn

© 2008 Chinese Physical Society and IOP Publishing Ltd

where C_s, ρ_s, K_s, α_b and R are the thermal capacity, the mass density, the thermal conductivity, and the absorption and reflection coefficients of the solid target, respectively. I is the intensity of laser light reaching the target surface.

We define the melting temperature T_m, and τ_m is the relaxation time that the target begins to melt; the thermal diffuse depth δ_m can be obtained from Ref. [12],

$$\tau_m = \frac{3(T_m - T_0)^2 C_s \rho_s K_s}{4 I_s^2}, \tag{2}$$

$$\delta_m = A\sqrt{\alpha \tau_m}, \tag{3}$$

where T_0 is the initial temperature of target, I_s is the laser intensity absorbed by the target surface, and α is the thermal diffusion coefficient. A is an alterable coefficient for different targets, for Si $A = 3.37$[6] and for Ni $A = 1$.[13] Based on the energy conservation law and the adiabatic condition, the boundary conditions can be expressed as

$$-K_s \frac{\partial T_s(x,t)}{\partial x}\Big|_{x=0} = (1-R)I(t),\ (0 < t < \tau_m), \tag{4}$$

$$-K_s \frac{\partial T_s(x,t)}{\partial x}\Big|_{x=d} = 0,\ (0 < t < \tau_m), \tag{5}$$

where d is the target thickness.

The time-dependent temperature distribution in the target depth $T(x,t)$ is governed by the heat-flow equation in one-dimensional form, proper to many experimental situations:[1]

$$C_l \rho_l \frac{\partial T}{\partial t} - C_l \rho_l V_r \frac{\partial T}{\partial x} = \frac{\partial}{\partial x}\Big(K_l \frac{\partial T}{\partial x}\Big) + (1-R)\alpha_b I(t)\exp(-\alpha_b x), \tag{6}$$

where C_l, ρ_l, K_l, α_b and R are the thermal capacity, the mass density, the thermal conductivity, and the absorption and reflection coefficients of the liquid target, respectively. I is the intensity of laser light reaching the target surface. The subscript l means that all the parameters are under the condition of liquid state. We also set the coordinate origin at the ablation surface.

The velocity of surface recession V_r is defined under the assumption that the flow of vaporized material from the surface follows the Hertz–Knudsen equation,[1,4,13] so the velocity of surface recession reads

$$V_r \approx \frac{P}{\rho(2\pi k_B T/m)^{1/2}}(1-\beta), \tag{7}$$

where P is the gas pressure, k_B is the Boltzmann constant, m is the particle average mass, and β is the fraction of the vaporized particle returning to the target surface (back flux). Generally, the β value varies from 0 in the weak-desorption regime to 0.2–0.3 in the regime of developed ablation.[2] Here we take $\beta = 0.18$, which is commonly used for stationary vaporization.[6,14] Under the limit $V_{\rm liq} \ll V_{\rm gas}$ ($V_{\rm liq}$ and $V_{\rm gas}$ are the molar volume of liquid and gas), we assume the inequality $T < T_{tc}$, where T_{tc} is the thermodynamic critical temperature.[1] Then, the relation between the equilibrium vapour press P and the temperature T may be computed from the Clausius–Clapeyron equation

$$P = P_b \exp\Big\{\frac{\Delta H_v(T_b) m}{k_B}\Big(\frac{1}{T_b} - \frac{1}{T}\Big)\Big\}, \tag{8}$$

where T is the temperature of target surface and P_b is 1 atm. ΔH_v is the heat of vaporization that we assume, as a first approximation, equal to the value at T_b (the boiling temperature at 1 atm).

The intensity of laser light reaching the target surface is written as

$$I(t) = I_0(t)\exp[-(\alpha_{\rm IB} + \sigma_{\rm PI} n_x)H], \tag{9}$$

where $I_0(t)$ is the incident laser intensity. The two dominant mechanisms for absorption of laser light are electron-ion and electron-neutral inverse bremsstrahlung (IB) and the photoionization of excited atoms (PI).[15] Here $\alpha_{\rm IB}$ is the IB inverse absorption length, $\sigma_{\rm PI}$ is the photoionization cross section, n_x is the number density of the excited neutral and H is the vapour height.[2] The details of $\alpha_{\rm IB}$ and $\sigma_{\rm PI}$ have been described in Ref. [16].

Based on the conservation of energy principle and continuous-temperature condition, we obtain the boundary condition at the surface, i.e.

$$-K_l \frac{\partial T_l(x,t)}{\partial x}\Big|_{x=0} = -\Delta H_v \rho_l V_r + (1-R)I_0(t) \cdot \exp[-(\alpha_{\rm IB} + \sigma_{\rm PI} n_x)H], \quad (\tau_m < t < \tau), \tag{10}$$

$$T(x,t)|_{t=\tau_m} = T'(x,t)|_{t=\tau_m}, \tag{11}$$

where $T'(x,t)|_{t=\tau_m}$ is the temperature distribution at the end of the melting stage.

Gaussian energy distribution is chosen as the laser pulse source. The laser wavelength is 266 nm, pulse width is 3 ns, and the initial temperature of the sample is 300 K. The thermal and optical properties of Si obtained from Ref. [6] are presented in Table 1.

Table 1. Thermal and optical properties of Si target.

K_s (J·[s·cm·K]$^{-1}$)	K_l (J·[s·cm·K]$^{-1}$)	ρ_s (g/cm^3)	ρ_l (g/cm^3)
1.35	0.6	2.32	2.53
ΔH_v (J/g)	R	C_s (J·g^{-1}·K^{-1})	C_l (J·g^{-1}·K^{-1})
13722.0	0.72	1.05	0.97

Firstly, we discuss the temperature evolution of target surface. The laser fluence is 10 J/cm^{-2}. In

Fig. 1, we present there are three curves that are the results without considering vaporization and plasma shielding and with considering vaporization but not plasma shielding and involving both the vaporization and the plasma shielding.

We can see from Fig. 1, at the beginning of the ablation ($t \leq \tau_m$), the results for three different models nearly overlap. The reason is that during this period, we have considered the relaxation time of vaporization. There is no vaporization that exists at the surface during this stage, so the energy loss of vaporization is negligible. However, during the time period of $\tau_m \leq t \leq \tau$, we can see that the temperature obtained from the model considering vaporization increases not as fast as that of the model which does not consider the vaporization, and the higher the surface temperature, the lower the rise rate of the surface temperature. We can analyse the phenomenon as follows: along with the temperature rising gradually, vaporization becomes more remarkable, and the energy loss at the surface becomes larger, which leads to the temperature decrease accordingly. Moreover, the temperature curve involving vaporization and plasma shielding rises slower. The reason is that with the time, more laser energy is absorbed by the plasma.

Meanwhile, the evolution of ablation rate under different laser irradiations is performed, which is presented in Fig. 2.

Figure 2 shows the profile of ablation rate versus irradiated time for different laser fluences. We note that the evolution of ablation rate has a nearly Gaussian shape. The two curves nearly overlap and on the verge of zero in the initial stage of ablation. That is vaporization relaxation stage. The higher the laser fluence, the shorter the vaporization relaxation time.

We can obtain the evolution of ablation depth by integrating the velocity of surface recession, as shown in Fig. 3. After a relaxation time, the ablation depth increases in the form of exponent. Uniformly, the higher the laser fluence, the shorter the vaporization relaxation time. It can be seen that the ablation depth reaches magnitude of μm. It shows that the vaporization is important in the ablation process, and it is indispensable.

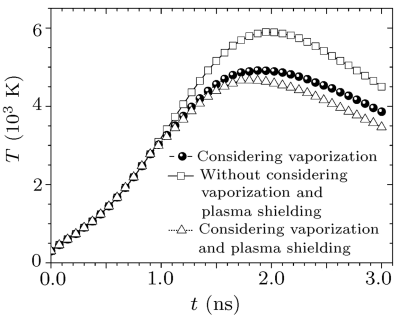

Fig. 1. Comparison of the evolution of surface temperature obtained from three different models.

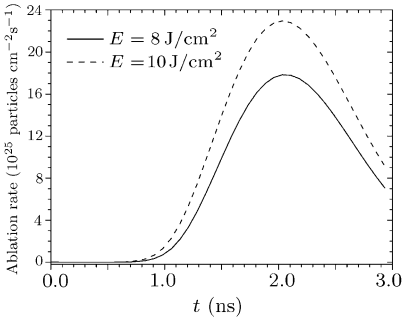

Fig. 2. Profile of the ablation rate versus irradiated time for different laser fluences.

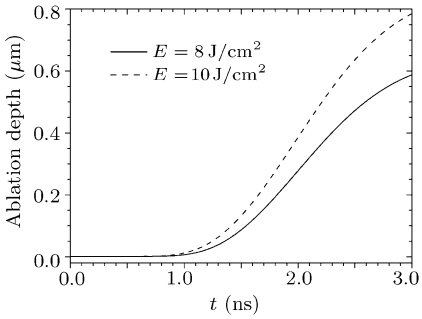

Fig. 3. Evolution of ablation depth for two different laser fluences.

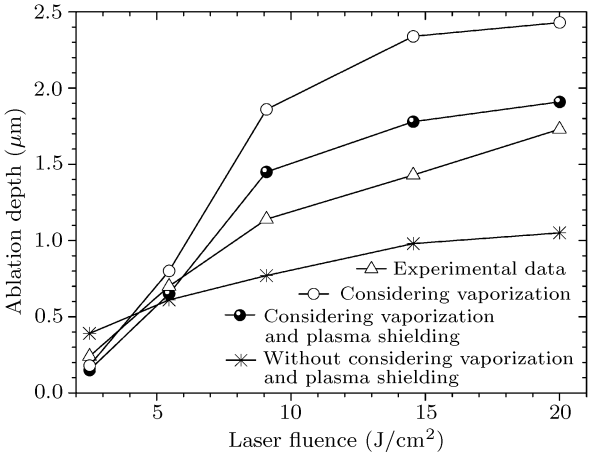

Fig. 4. Comparison between the experimental data and the simulated results for three models.

Finally, we describe the behaviour of the ablation depth versus laser fluence in Fig. 4. The experimental data come from Ref. [2]. In this figure, the first curve is obtained with vaporization. The second curve is based on the model without considering vaporization and plasma shielding. Considering the vaporization effects and plasma shielding, we simulate the third curve. It is clear that our model is more proper to describe the ablation process. That is to say, plasma shielding plays a relevant role in the ablation process.

Besides simulating the Si target, we simulate the metal target. In this study, we select a Ni target.

In the experiment we employ a laser at wavelength 248 nm and pulse width 25 ns (FWHM). The centre, uniform portion of the excimer laser beam, is passed through a rectangular aperture (10 mm by 5 mm) to produce a laser beam with a uniform intensity profile. A single 150 mm focal length CaF_2 lens is used to focus the laser beam on the target. Polished nickel (50 nm rms roughness) is used as the target.

Details of the experiments have been given elsewhere.[13] Accordingly, we consider the temperature-averaged values of Ni thermophysical

properties, and they are obtained from Ref. [10], presented in Table 2.

Table 2. Thermal and optical properties of Ni target.

Thermal conductivity ($J \cdot s^{-1} \cdot cm^{-1} \cdot K^{-1}$)	0.9
Special heat ($J \cdot g^{-1} \cdot K^{-1}$)	0.44
Enthalpy of vaporization (J/kg)	6453.2
Density (g/cm^3)	8.9
Nickel reflectivity	0.7255
Absorption coefficient (m^{-1})	6.138×10^7

In Fig. 5, the comparison of evolution of transmitted intensity with the experimental data is performed. The plasma is formed after the relaxation time. During this period, the transmitted intensity equals one. Because of the plasma absorbing the laser energy, the transmitted intensity gradually decreases. Moreover, at higher laser fluences, for laser-target stronger interaction, the relaxation time is shorter and the transmitted intensity decreases faster. Our numerical results are in good agreement with the experimental data.

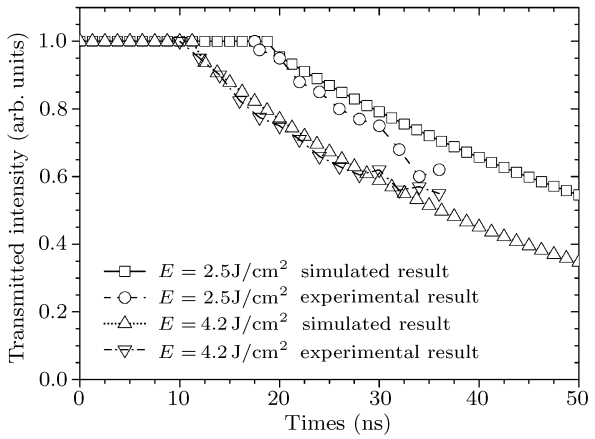

Fig. 5. Comparison of the evolution of transmitted intensity with the experimental data for two laser energies.

Figure 6 shows the variation of ablation depth per pulse with laser fluence. The experimental data comes from Ref. [13]. In this figure, three simulated results on different models are shown. It can be seen that our numerical results are more in agreement with the experimental data, especially for higher laser fluence.

The effect of plasma absorption in controlling the ablation characteristics is qualitatively investigated. In this study, the thermal model for nanosecond laser sputtering at high fluences is performed, involving both the vaporization and the plasma shielding. (a) As an example of Si target, we obtain the time evolution of the calculated surface temperature, ablation rate and ablation depth by solving the heat flow equations using a finite difference method. At the same time, under different conditions the ablation depth with laser fluence is shown. It can be seen that vaporization and plasma shielding are prominent in the ablation process with time. (b) At the same time, we simulate the pulsed laser irradiation Ni target, the evolution of the transmitted intensity and the variation of ablation depth per pulse with energy density are performed. Our numerical results are more consistent with the experiment data. The result shows that plasma shielding plays a relevant role in the ablation process.

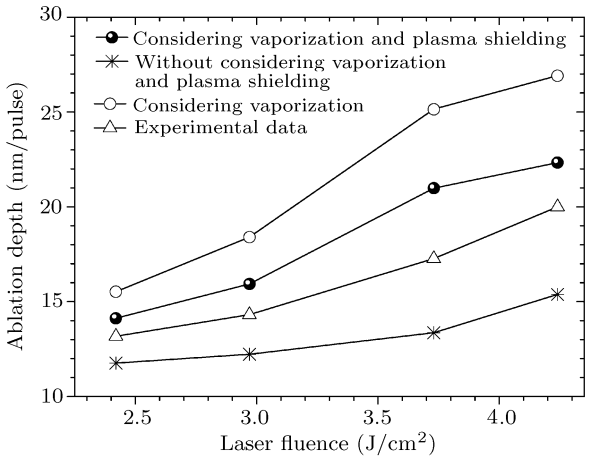

Fig. 6. Comparison between the experimental data and the simulated results for three models.

Our modified ablation depth formula improves the existing ablation theory of pulsed laser deposition, which is very important for further investigation of the PLD technique.

References

[1] Peterlongo A, Miotello A and Kelly R 1994 *Phys. Rev.* E **50** 4716
[2] Yoo J H, Jeong S H and Russo R E 2000 *J. Appl. Phys.* **88** 1638
[3] Craciun V and Craciun D 1999 *Appl. Surf. Sci.* **138/139** 218
[4] Kelly R and Miotello A 1996 *Appl. Surf. Sci.* **96/98** 205
[5] Lu Q M, Mao S and Mao X L 2002 *Appl. Phys. Lett.* **80** 3072
[6] Tan X Y and Zhang D M 2005 *Physica* B **358** 86
[7] Zhang D M and Li Z H 2001 *Ceramic Bulletin* (U.S.) **80** 57
[8] Zhang D M, Guan L and Li Z H 2003 *Acta Phys. Sin.* **52** 242 (in Chinese)
[9] Lunny J G and Jordan R 1998 *Appl. Surf. Sci.* **127–129** 941
[10] Willis D A and Xu X F 2002 *Int. J. Heat Mass Transfer* **45** 3911
[11] Li Z H and Zhang D M 2002 *Chin. Phys. Lett.* **19** 1841
[12] Zhang D M, Hou S P and Guan L 2004 *Acta Phys. Sin.* **53** 209 (in Chinese)
[13] Xu X F and Willis D A 2002 *J. Heat Transfer* **124** 293
[14] Bulgakova N M, Bulgakov A V and Babich L P 2004 *Appl. Phys.* A **79** 1323
[15] Zel'dovich Ya B and Raizer Yu P 1966 *Physics of Shock Waves and High-Temperature Hydrodynamics Phenomena* (New York: Academic) vol 1
[16] Zhang D M, Liu D and Li Z H 2005 *Physica* B **362** 82